

Realization of Low-frequency Amplitude Modulator and Demodulator with FPAA's

Ivailo Pandiev¹

Abstract – This paper presents a low-frequency amplitude modulator and demodulator based on Field Programmable Analogue Array (FPAA) devices. For creating the FPAA circuits, amplitude modulation and synchronous demodulation methods known from designing analogue RF transmission systems have been adapted. The proposed system allows redesigning the analogue conditioning stage thanks to the use of a FPAA device, which may be adapted to the requirements of the signal shape and the electrical parameters. For a sinusoidal carrier signal the amplitude modulation (AM) is performed with multiplier, while for a square-wave carrier signal, switch is employed instead of multiplier. In the synchronous demodulation the modulated carrier sinusoidal signal is multiplied by an unmodulated carrier signal with the same frequency and phase. For a square-wave carrier signal in the demodulation process the multiplier is replaced with switch, controlled by square-wave signal. The functional elements of the structures are realized by employing available configurable analogue modules (CAMs) of the FPAA's AN231E04 and AN220E04 from Anadigm. The FPAA circuits can operate with single supply voltage of +3,3V and +5V, respectively. The simulation and experimental results show good agreement with the theoretical predictions.

Keywords – Analogue circuits, Amplitude modulation, Synchronous demodulation, FPAA, System prototyping.

I. INTRODUCTION

Low-frequency useful information can be conveyed by amplitude modulation (AM) of a high-frequency carrier wave. Many naturally occurring sounds are modulated in both amplitude and frequency. The speech and other specific communication signals in mammals, marine species and birds include amplitude and frequency modulation components. The ability to detect fluctuations in the amplitude and frequency of sounds is considered as important for normal auditory processing, including the perception of speech. Recently, several studies have been reported in the literature [1-5]. The majority of the papers contain analyses of human speech or present computer based approaches for detection of sinusoidal amplitude modulation components. Moreover, those schemes cannot be used to realize monolithic electronic systems implementing low-frequency amplitude modulation and demodulation. Without any doubt low-frequency amplitude modulators and demodulators are necessary for analog signal processing of the natural sounds. However, powerful low-frequency modulators and demodulators have not been available yet. This paper introduces new low-frequency amplitude

modulators and demodulators based on Field Programmable Analogue Arrays (FPAA's). The FPAA integrated circuits (ICs) are flexible, economical and fast prototyping solutions for the design of complex analogue acquisition systems [6-8]. In particular FPAA's are basically suitable for signal conditioning, gain, filtering, summing and multiplying.

II. PRINCIPLE OF AMPLITUDE MODULATOR AND DEMODULATOR OPERATION

A. Modulation

In amplitude modulation (AM), the useful signal $u_S(t)$ modulates the amplitude of the carrier signal $u_C(t)$, while the phase of the carrier signal remains constant:

$$u_{AM}(t) = [U_{Cm} + u_S(t)] \cos \omega_C t \tag{1}$$

For AM with carrier signal, the sinusoidal modulating signal

$$u_S(t) = U_{Sm} \cos \omega_S t \tag{2}$$

renders a modulated signal

$$\begin{aligned} u_{AM}(t) &= [U_{Cm} + U_{Sm} \cos \omega_S t] \cos \omega_C t = \\ &= \underbrace{U_{Cm} \cos \omega_C t}_{u_C(t)} + \underbrace{\frac{K_{AM} U_{Cm}}{2} \cos(\omega_C - \omega_S)t}_{u_{LSB}(t)} + \\ &\quad + \underbrace{\frac{K_{AM} U_{Cm}}{2} \cos(\omega_C + \omega_S)t}_{u_{USB}(t)}, \end{aligned} \tag{3}$$

where $K_{AM} = U_{Sm} / U_{Cm}$ is the modulation depth (≤ 1).

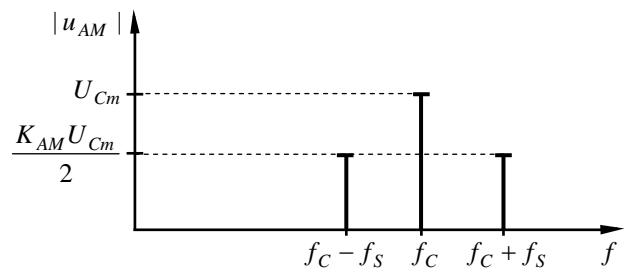


Fig. 1. Spectra of a modulated carrier with sinusoidal signal.

The modulated carrier signal consists of the *unmodulated carrier signal* $u_C(t)$, a useful signal $u_{LSB}(t)$ at the frequency $f_C - f_S$ in the *lower sideband* and a useful signal $u_{USB}(t)$ at

¹Ivailo Pandiev is with the Faculty of Electronics at Technical University of Sofia, 8 Kl. Ohridski Blvd, Sofia 1000, Bulgaria, E-mail: ipandiev@tu-sofia.bg.

the frequency $f_C + f_S$ in the upper sideband. Fig. 1 shows the spectra of the modulated carrier signal.

To produce an amplitude-modulated signal according to (1), it is necessary to use a multiplier and a sinusoidal carrier signal $u_C(t) = U_{Cm} \cos \omega_C t$. Amplitude modulator with multiplier is shown on Fig. 2.

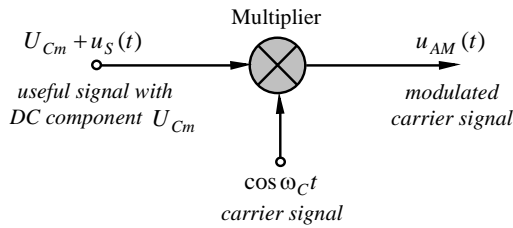


Fig. 2. Amplitude modulator with multiplier.

Instead of the sinusoidal carrier signal $\cos \omega_C t$, a square-wave signal with amplitude levels 0 and 1 and period length $T_C = 1/f_C$ can be used. In this case the multiplier has to be replaced with a switch [9]. From the Fourier series of the symmetrical (pulse duty ratio is equal to 50%) square-wave signal can be seen that besides the desired carrier with frequency f_C , other carrier components also occur with frequency equal to the carrier frequency f_C and multiplied by an odd integer (3, 5, etc.):

$$u_C(t) = \begin{cases} 1 & \text{for } nT_C \leq (n+1/2)T_C \\ 0 & \text{for } (n+1/2)T_C < (n+1)T_C \end{cases} \quad n \text{ integer}$$

$$= \frac{1}{2} + \frac{2}{\pi} \cos \omega_C t - \frac{2}{3\pi} \cos 3\omega_C t + \frac{2}{5\pi} \cos 5\omega_C t \dots$$

$$= \frac{1}{2} + \frac{2}{\pi} \sum_{n=0}^{\infty} \frac{(-1)^n}{2n+1} \cos(2n+1)\omega_C t. \quad (4)$$

In the output resulting signal each components of Eq. (4) is modulated by the useful signal and has the corresponding sidebands. The desired carrier signal with its sidebands has to be extracted from this mixture with band-pass filter. On Fig. 3 amplitude modulator with switch and output band-pass filter is shown.

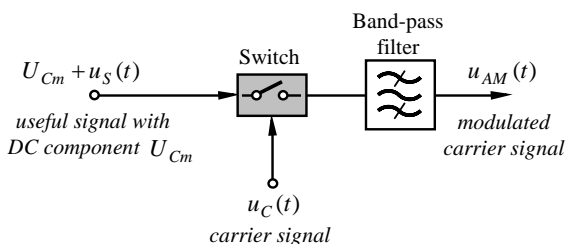


Fig. 3. Amplitude modulator with switch [9].

B. Demodulation

There are two basic types of electronic circuits, which realize amplitude demodulation: (1) envelope detector and (2)

synchronous demodulator. In general the envelope detectors consist of a peak-type rectifier and a high-pass filter for rejecting the DC component [10]. The main advantage of the envelope detector is its simple design. A drawback is the nonlinearity of the transfer characteristic due to the nonlinear I-V characteristic of the diodes within the peak-type rectifier, especially at smaller amplitude of the carrier signal. The envelope detectors are used basically in the AM radio receivers.

Higher quality of the demodulation process can be achieved by synchronous demodulation, although this requires much more complex electronic circuit. In this demodulation method, the modulated carrier signal is multiplied by an unmodulated carrier signal with the same frequency and the same phase. For sinusoidal modulated signal this results in:

$$u_D(t) = u_{AM}(t) \cos \omega_C t =$$

$$= [U_{Cm} + U_{Sm} \cos \omega_S t] \cos \omega_C t \cos \omega_C t =$$

$$= [U_{Cm} + U_{Sm} \cos \omega_S t] \frac{1 + \cos 2\omega_C t}{2} =$$

$$= \frac{U_{Cm}}{2} + \frac{U_{Cm}}{2} \cos 2\omega_C t + \frac{U_{Sm}}{2} \cos \omega_S t +$$

$$+ \frac{U_{Sm}}{4} \cos(2\omega_C - \omega_S)t + \frac{U_{Sm}}{4} \cos(2\omega_C + \omega_S)t. \quad (5)$$

Besides the required component $U_{Cm} + U_{Sm} \cos \omega_S t$ the signal product $u_D(t)$ also contains additional components of 1/2 weighting in the double carrier frequency range. Those components can be suppressed by a low-pass filter. The synchronous demodulator circuit is shown in Fig. 4. For demodulation of the modulated signal with square-wave signal the multiplier in Fig. 4 has to be replaced with a switch [9]. In this case the modulated signal is multiplied with square-wave signal with a period length $T_C = 1/f_C$. The resulting additional components in the signal product $u_D(t)$ are also suppressed by a low-pass filter.

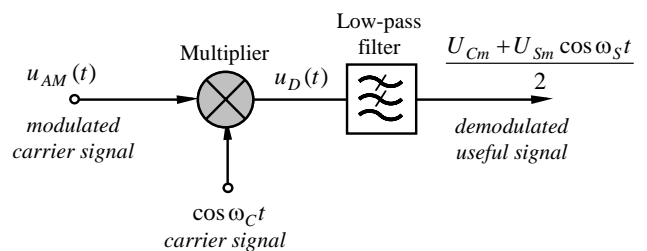


Fig. 4. Synchronous demodulator.

The synchronous demodulator with multiplier or switch largely corresponds to the amplitude modulator with multiplier or switch shown in Fig. 2 and Fig. 3, respectively. They differ only with regard to the necessary filters.

The use of a switch in the modulator requires additional band-pass filter in order to suppress unwanted (high-frequency) signal components. The low-pass filter in the synchronous demodulator is always required, regardless of whether a multiplier or a switch is used.

III. FPAA FOR LOW-FREQUENCY AMPLITUDE MODULATION AND DEMODULATION

This section analyzes the suitability of FPAA for low-frequency amplitude modulation and demodulation. A subsequent presentation of the Anadigm® FPAA architecture and functionalities [11] allows to link them with those required for conditioning of analogue signals with small amplitude and wide bandwidth.

The synthesis of the analogue system for modulation and demodulation is strongly conditioned by the incoming signal features, such as amplitude, frequency and noise level. This means that the implementation of the circuit would have to allow change the multiplication factor when variation in the signal amplitude occur and it should be able to change the pole (centre) frequency of the filters for different noise levels. These requirements are easily achieved using a FPAA to synthesize this analogue system. The basic advantages of the FPAA ICs offered by Anadigm are:

- Dynamically programmable parameters “on-the-fly”;
- Offer a tradeoff between performance and system design time;
- Possibility for realization of complex analogue or mixed function without external passive components.

The main drawback presented by the use of FPAAs could be their high power consumption, compared with that of some ASICs. This drawback is affordable for implementations that are intended to be a portable instrument.

IV. FPAA CONFIGURATIONS FOR LOW-FREQUENCY AMPLITUDE MODULATION AND DEMODULATION

Once the FPAAs features have been presented, this section is focused on the key qualities and elements of those devices that will be used for amplitude modulation and demodulation. Moreover, the functional circuits of voltage-mode low-frequency modulator and demodulator based on FPAA AN231E04 [12] and AN220E04 [13] are presented.

FPAA configuration of amplitude modulator and demodulator with multiplier based on AN231E04 is shown on Fig. 5. The differential input useful signal is connected to the FPAA input cell 1 (pins 01 and 02). In bypass mode, the input signal is routed directly through the cell, bypassing all active circuit elements. The output differential modulated carrier signal is obtained by the output cell 6 (pins 17 and 18). In bypass mode, the cell's output pins are being driven directly by the low-pass filter connected to the output cell. The carrier sinusoidal signal is generated by internal oscillator, which output in connected to node $n2$. The oscillator is realized by using *OscillatorSine* CAM. The oscillating frequency range is from 10kHz to 20kHz and the output amplitude is equal to 1V. The chip clock frequency of the oscillator is *Clock 3* with value 250kHz. For the synchronous demodulator the input modulated carrier signal can be applied to the output cell 3 (pins 11 and 12) and the corresponding output demodulated signal is obtained by the output cell 7 (pins 19 and 20). Furthermore the demodulation process is synchronized with carrier signal, generated by the *OscillatorSine* CAM.

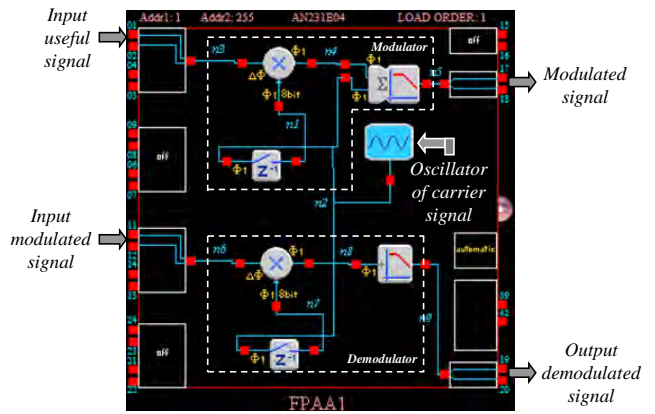


Fig. 5. FPAA configuration of amplitude modulator and synchronous demodulator with multiplier shown on Fig. 2 and Fig. 4, respectively.

FPAA configuration of amplitude modulator and demodulator with switch based on AN220E04 is shown in Fig. 6. The differential input unmodulated signal is connected to the FPAA input cell 1 (pins 09 and 10) and the output modulated signal is obtained by output cell 1 (pins 03 and 04). In the modulator with switch for realization of the switch is used a *GainSwitch* CAM. This CAM creates a gain stage with two switchable input terminals. The useful signal is applied to the upper input with $G1 = -1$ and the signal ground ($V_{MR} = +2V$ (Voltage Mid-Rail - VMR)) is connected to the lower input with $G2 = +1$. Selection of the two inputs is controlled through a comparator, which is part of this CAM. This comparator has options similar to those of the *Comparator* CAM including the ability to select what the Control signal will be compared to. The carrier square-wave signal is generated by internal oscillator, realized by using *OscillatorTriSqr* CAM. The desired modulated carrier signal is extracted with band-pass *FilterBiquad* CAM. The corner frequency is equal to f_s and quality factor is $Q \approx f_c / 2f_s$. For the synchronous demodulator with switch the input modulated signal is applied to the output cell 3 (pins 37 and 38) and the corresponding output demodulated signal is obtained by the output cell 2 (pins 07 and 08). The switch within the demodulator is realized with second *GainSwitch* CAM. The unwanted signal components are suppressed with low-pass *FilterBilinear* CAM.

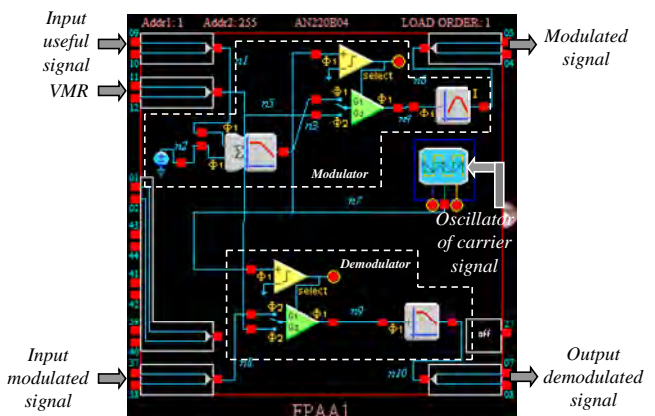


Fig. 6. FPAA configuration of amplitude modulator and demodulator with switch shown on Fig. 3 and Fig. 4 (the multiplier on Fig. 4 has to be replaced with a switch), respectively.

V. SIMULATION AND EXPERIMENTAL RESULTS

VI. CONCLUSION

The workability of the proposed amplitude modulator and demodulator of Fig. 5 and 6 is presented by the simulation results using the simulator built in *AnadigmDesigner2* and also through the experimental results from the circuit configured on prototype board. The experimental test that has been used for validating the FPAA configuration shown on Fig. 5 is based on the AN231K04-DVLP3 – Development Board, which is built around the AN231E04 device.

The input and output waveforms of the FPAA configuration shown on Fig. 5 at carrier frequency $10kHz$ are illustrated on Fig. 7 and Fig. 8. The amplitude modulation of a useful sinusoidal signal with amplitude $500mV$ and frequency $500Hz$ is presented on Fig. 7. The demodulation process of the modulated carrier signal is shown on Fig. 8. The original unmodulated signal has amplitude $500mV$ and frequency $500Hz$. The goal of a 2% match between the simulation model, built in *AnadigmDesigner2* and the actual device was achieved.

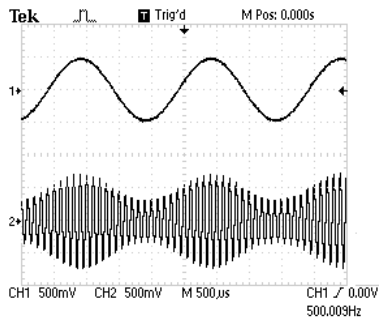


Fig. 7. Modulated signal – CH2 (single-ended – pin 17 on FPAA AN231E04) with carrier at sin-wave – CH1 ($K_{AM} = 0,5$).

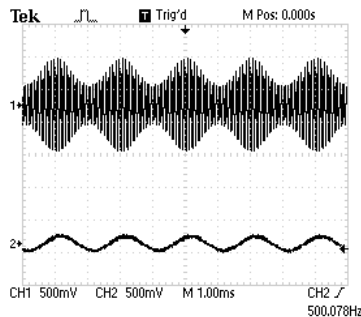


Fig. 8. Demodulated signal – CH2 (single-ended – pin 19 on FPAA) at AM with carrier – CH1 and $K_{AM} = 0,5$.

The input and output waveforms of the FPAA configuration on Fig. 6 at square-wave carrier $10kHz$ are shown on Fig. 9.

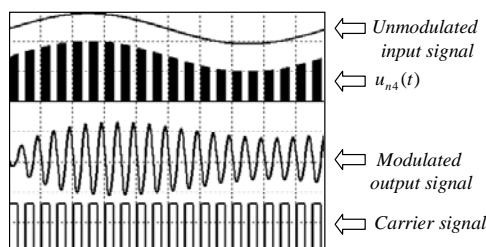


Fig. 9. Simulation results of the FPAA configuration on Fig. 6. The horizontal scale is $200\mu s / div$ and the vertical scale is $2V / div$.

In this paper a low-frequency amplitude modulator and demodulator by using of a synchronous modulation and demodulation method has been proposed. The amplitude modulation circuit consists of a multiplier (or a switch and band-pass filter for a square-wave carrier signal). The synchronous demodulator circuit with multiplier or switch largely corresponds to the amplitude modulator with multiplier or switch. They differ only as regard to the necessary filters. The selected FPAA's are an Anadigm AN231E04 and AN220E04, where the analogue signal processing is implemented. The experimental and simulation results, obtained for various input signals confirm the theoretical analysis.

ACKNOWLEDGEMENT

This paper is sponsored by the research program of the Technical University of Sofia, Bulgaria.

REFERENCES

- [1] H. Li, T. Li, "Generalized multichannel amplitude-and-phase coded modulation for differential space-time communications", *Digital Signal Processing*, vol. 17, pp. 261-271, 2007.
- [2] I-H. Hsieh, K. Saberi, "Detection of sinusoidal amplitude modulation in logarithmic frequency sweeps across wide regions of the spectrum", *Hearing Research*, vol. 262, pp. 9-18, 2010.
- [3] A. Qayoum, V. Gupta, P. Panigrahi, K. Muralidhar, "Influence of amplitude and frequency modulation on flow created by a synthetic jet actuator", *Sensors and Actuators A*, vol. 162, pp. 36-50, 2010.
- [4] K. Banai, A. Sabin, B. Wright, "Separable developmental trajectories for the abilities to detect auditory amplitude and frequency modulation", *Hearing Research*, vol. 280, pp. 219-227, 2011.
- [5] G. Prendergast, S. Johnson, G. Green, "Extracting amplitude modulations from speech in the time domain", *Speech Communication*, vol. 53, pp. 903-913, 2011.
- [6] E. Manolov, P. Yakimov, M. Hristov, "Controllable square-wave generators by using FPAA", *Elektrotechnica & Elektronica E+E*, No 11-12, pp. 3-7, 2004 (in Bulgarian).
- [7] Zh. Georgiev, E. Manolov, T. Todorov, I. Karagineva, "Synthesis and Experimental Verification of Sinusoidal Oscillator Based on the Modified Van der Pol Equation", *Inter. Journal of Electronics*, vol. 96, No 5, pp. 467-478, 2009.
- [8] D. Morales, A. Garcia, E. Castillo, M. Carvajal, J. Banqueri, A. Palma, "Flexible ECG acquisition system based on analog and digital reconfigurable devices", *Sensors and Actuators*, vol. 165, pp. 261-270, 2011.
- [9] V. Tietze, Ch. Schenk. *Electronic circuits*. 2nd Edition. Berlin, Heidelberg, New York. Springer-Verlag, 2008.
- [10] M. Seifart. *Analoge Schaltungen*. 6 Auflage. Verlag Technik Berlin, 2003 (in German).
- [11] The Anadigm Product Range, <http://www.anadigm.com/products.asp>, last accessed January 25, 2012.
- [12] AN231E04 Datasheet – Dynamically Reconfigurable dpASP, <http://www.anadigm.com/an231e04.asp>, last accessed January 25, 2012.
- [13] AN220E04 Datasheet – Dynamically Reconfigurable FPAA, <http://www.anadigm.com/an220e04.asp>, last accessed January 25, 2012.